



Cite this: *RSC Adv.*, 2021, **11**, 10794

# Preparation and characterization of enzymatically cross-linked gelatin/cellulose nanocrystal composite hydrogels

Yaqi Dong, Shouwei Zhao, Wenhui Lu, Nan Chen, Deyi Zhu \* and Yanchun Li\*

Gelatin is an attractive hydrogel material because of its excellent biocompatibility and non-cytotoxicity, but poor mechanical properties of gelatin-based hydrogels become a big obstacle that limits their wide-spread application. To solve it, in this work, gelatin/cellulose nanocrystal composite hydrogels (Gel-TG-CNCs) were prepared using microbial transglutaminase (mTG) as the crosslinking catalyst and cellulose nanocrystals (CNCs) as reinforcements. The physicochemical properties of the composite hydrogels were investigated by thermogravimetric analysis (TGA), X-ray diffraction (XRD) and scanning electron microscopy (SEM). The dynamic rheological measurement and uniaxial compression test were performed to study the effects of mTG and CNC contents on the storage modulus and breaking strength of the as-prepared Gel-TG-CNCs. Results showed that the addition of CNCs and mTG could significantly increase the storage modulus and breaking strength of gelatin-based hydrogels, especially when added simultaneously. The breaking strength of Gel-TG-CNCs (2%) at 25 °C can reach 1000 g which is 30 times greater than pure gelatin hydrogels. The biocompatibility of the composite hydrogels was also investigated by the MTT method with Hela cells, and the results demonstrated that the composite hydrogels maintained excellent biocompatibility. With a combination of good biocompatibility and mechanical properties, the as-prepared Gel-TG-CNCs showed potential application value in the biomedical field.

Received 4th February 2021  
Accepted 8th March 2021

DOI: 10.1039/d1ra00965f

rsc.li/rsc-advances

## 1. Introduction

Hydrogels are mainly formed by synthetic or natural polymers through physical, chemical or enzymatic methods and have a stable 3D network structure, which can absorb and retain a large amount of aqueous solutions.<sup>1,2</sup> Due to their tunable properties, considerable biocompatibility, and similarity with tissue and cell environments, hydrogels have demonstrated great potential as one of the most promising groups of biomaterials.<sup>3,4</sup> Especially in the biomedical field, hydrogels have been used for a wide range of medical applications such as drug and gene delivery, synthetic extracellular matrix and as scaffolds for tissue engineering.<sup>5</sup> Nevertheless, for biomedical use, the hydrogel components must be safe and compatible with the biological system. Thus, the utilization of biocompatible and biodegradable biopolymers (cellulose, gelatin, chitosan, hyaluronic acid, *etc.*) has been widely accepted in the design of hydrogels.<sup>6,7</sup>

Among these biopolymers, gelatin is an attractive candidate as starting material for bio-hydrogel preparation thanks to its non-cytotoxicity, good biocompatibility, low antigenicity, easy

degradation and unique gelling properties.<sup>8</sup> Gelatin is a proteinaceous material obtained by partial hydrolytic degradation of naturally occurring collagen, which is known to be the most abundant protein in mammals.<sup>9</sup> Furthermore, gelatin contains abundant functional groups including the amino and carboxyl groups on its side chain, amenable to various types of chemical modifications.<sup>10</sup> This offers the opportunity to introduce cross-linkage or bioactive moieties into the backbone of hydrogels. However, the main disadvantages of gelatin-based hydrogel are poor mechanical stability and durability, which critically limit their wide-spread applications.<sup>11</sup>

Therefore, the manufacture of gelatin-based hydrogels frequently requires a certain degree of crosslinking for stabilizing gelatin peptides. Several approaches for crosslinking gelatin have been used, such as physical crosslinking, chemical crosslinking and enzymatic crosslinking.<sup>12</sup> Amongst, physical crosslinking methods by using ultraviolet radiation, plasma treatment and dehydro-thermal techniques usually have low crosslinking extent of gelatin macromolecules, which are attributed to the lack of control over crosslink density. As for chemically crosslinking, the residual of chemical cross-linkers and organic solvents often cause either cytotoxic side-effects or immunological responses from the host. Enzymatic crosslinking method has received more and more attention due to its low cytotoxicity and milder reactions.<sup>13</sup> Microbial

School of Light Industry and Engineering, Qilu University of Technology (Shandong Academy of Sciences), Jinan 250353, China. E-mail: zhdy@qlu.edu.cn; qlulyc@126.com



transglutaminase (mTG) can catalyze the acyl-transfer reaction between the  $\epsilon$ -amino group of lysine and the  $\gamma$ -carboxamide group of glutamines in proteins.<sup>14</sup> Meanwhile, it can catalyze the transfer of amide bonds within and between protein molecules, thereby promoting the formation of hydrogel from gelatin solution. It was shown previously that gelatin hydrogel crosslinked by mTG exhibits excellent performance in cell adhesion, proliferation, and differentiation.

However, either by the means of chemical or enzymatic crosslinking, the cross-linking points in gelatin hydrogel networks form randomly, causing variations in crosslink density that resulted in stress concentration on the least extensible chains under deformation.<sup>15</sup> These factors make gelatin hydrogels reinforcement undesirable, such as, brittleness, limited elongation, and lack of toughness. Based on a multiphase composite theory, special nanoparticles have been introduced as strengthening agent to overcome the irregular distribution of the cross-linking points of chemically cross-linked hydrogels.<sup>16</sup> Thus, a strong hybrid polymer network can be formed by physical or chemical association between nanoparticles and polymer chains. Recently, one-dimensional nanomaterials such as carbon nanotubes (CNTs),<sup>17–19</sup> and two-dimensional nanomaterials such as clay nanosheets, graphene and silicate nanoparticles have been integrated into gelatin-based hydrogels to enhance the mechanical performance of these materials.<sup>20</sup>

Cellulose nanocrystals (CNCs), an abundant natural nanomaterial, have been also employed as the reinforcing agent for synthetic or natural polymer hydrogels, due to their excellent mechanical properties, biocompatibility, biodegradability, renewability and non-toxicity.<sup>21</sup> According to the study from Dash *et al.*, oxidized cellulose nanowhiskers can obviously improve the mechanical and thermal properties of gelatin hydrogel by increasing chemical cross-linking junction points between gelatin and nanowhiskers.<sup>22</sup> Kevin *et al.* reported that CNCs are incorporated into hydrogels at concentrations of 0.1–5 wt% based on total swollen gel weight, the shear storage modulus of the hydrogels ( $G'$  as high as 60 kPa) can be increased by 35 times.<sup>23</sup>

Based on the above-mentioned advantages of CNCs and mTG, in this study, Gel-TG-CNCs hydrogels were prepared by enzymatic cross-linking CNCs and mTG, and the influence of CNCs content on the performance of hydrogels including the morphology, mechanical, and rheological were studied. The cytotoxicity, swelling and biocompatibility properties of the hydrogel were evaluated as well.

## 2. Materials and methods

### 2.1. Materials

Commercial CNCs solution was supplied by Zhongshan NanoFC Bio Materials Co., Ltd. Commercial porcine skin gelatin (type A, 300 Bloom), dulbecco's modified eagle's medium (DMEM) and cytotoxicity studies using Hela cells were purchased from Sigma Aldrich suppliers. Sodium hydrogen phosphate, citric acid, fetal bovine serum (FBS) and fluorescein diacetate (FDA) were purchased from Shanghai Macklin Biochemical Co., Ltd. Microbial transglutaminase (mTG) was obtained from Yiming Biotechnology Company ( $>100 \text{ U g}^{-1}$ , Jiangsu Province, China). All other chemicals used in the present study were of analytical grade or of higher quality and available locally and all solutions were prepared with deionized water.

### 2.2. Synthesis of Gel-TG-CNCs hydrogels

Gelatin was soaked in deionized water at room temperature for 2 h and then transferred to  $50^\circ\text{C}$  water bath to prepare 6.67% (w/v) gelatin solution. CNCs was sufficiently dispersed in deionized water by means of a high-speed disperser. The two solutions were mixed thoroughly in a glass beaker and the pH of mixed solution was adjusted to 6.5 with  $1.0 \text{ mol L}^{-1}$  NaOH. Enzyme-mediated cross-linking was carried out at  $50^\circ\text{C}$  for 60 min by adding  $10 \text{ U mTG g}^{-1}$  gelatin followed by a heating step of  $95^\circ\text{C}$  for 5 min to inactive the mTG. A series of gelatin/CNCs hydrogels (Gel-TG-CNCs) with different CNCs contents (0%, 0.5%, 1%, 1.5% and 2%) were prepared and named Gel-TG, Gel-TG-CNCs (0.5%), Gel-TG-CNCs (1%), Gel-TG-CNCs (1.5%) and Gel-TG-CNCs (2%) respectively. Fig. 1 represents

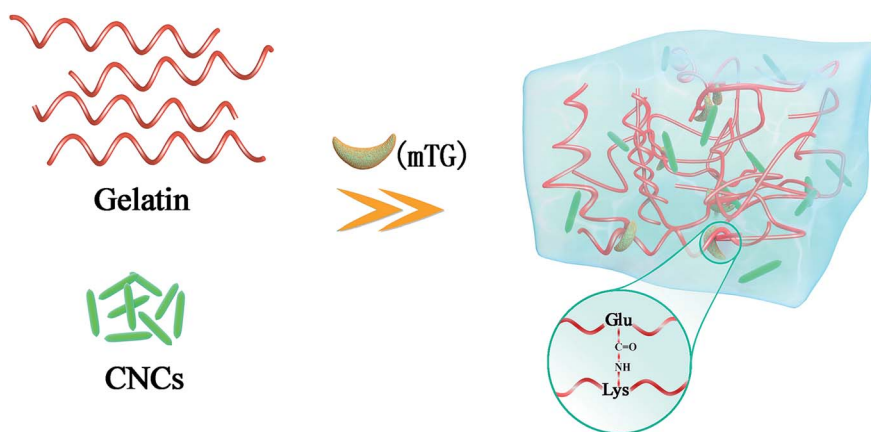


Fig. 1 Schematic illustration of the fabrication of gelatin/CNCs hydrogel.

the preparation process of Gel-TG-CNCs hydrogels. To well study the effect of mTG cross-linking, we also prepared the control hydrogels (Gel and Gel-CNCs (2%)) by refrigerating the gelatin or gelatin/CNCs solutions at 10 °C for 24 h. All of the samples have the same final gelatin concentration.

### 2.3. Thermostability analysis

Thermogravimetric measurements were performed by using a TGA (TGA 1 Mettler Toledo, Switzerland). Freeze-dried samples were placed in alumina crucibles and used an empty alumina crucible as a reference. Dynamic tests were run from 45 to 800 °C at a heating rate of 10 °C min<sup>-1</sup> under flowing nitrogen atmosphere.<sup>23</sup> The sample weight loss as function of temperature was recorded continuously.

### 2.4. XRD analysis

The crystal structure of CNCs, gelatin, and the gelatin/CNCs composite hydrogel were characterized by XRD. X-ray diffraction analyses were carried out on a D8 Powder X-ray Diffractometer (Rigaku Corporation, Japan) at a current of 40 mA and an accelerating voltage of 40 kV. Data were recorded in the range (2θ) of 5–60° with a scanning rate of 6° min<sup>-1</sup>.

### 2.5. Rheological behavior

The rheological behaviors of the Gel-TG and Gel-TG-CNCs hydrogels were analyzed in dynamic mode with a rotational rheometer (ARES/G2 TA Instruments, US), equipped with a 20 mm plate with diameter at a gap of 0.8 mm. The dynamic frequency scanning was performed at different temperatures (5 °C, 15 °C, 25 °C) with an angular frequency range of 0.0628 to 62.8 rad s<sup>-1</sup>, at constant strain of 0.5%. The storage modulus value of the sample (*G'*) with frequency were recorded and all experiments were performed within the linear viscoelastic region.

For the viscosity measurements, a 40 mm plate diameter was used with a gap distance set at 0.8 mm. All experiments were conducted at 25 ± 0.1 °C. The hydrogel sample was held on the plate, the shear rate was ramped from 0.1 to 100 L s<sup>-1</sup>. The curve of apparent viscosity was plotted *versus* shear rate. This research work provides examples of typical data, not averages.

### 2.6. Determination of gel strength

The gel strength was measured using a texture analyser (TA.XTplus, Stable Micro System, UK) equipped with a cylinder probe (P/0.5). The hydrogel samples were refrigerated at 5 °C for 24 h. Compression was applied with a load cell of 5 kN at a speed of 1.5 mm min<sup>-1</sup> at 25 °C.

### 2.7. Scanning electron microscopy (SEM)

The surface morphology of the hydrogel samples was evaluated using scanning electron microscopy (Phenom Pure<sup>+</sup>, Phenom world, Netherlands) at an acceleration voltage of 10 kV. In brief, to prepare samples for SEM, the hydrogels were broken in liquid nitrogen after being dried by lyophilization.

### 2.8. Swelling behavior

The hydrogel samples were cut into cylinder of 2.0 cm in diameter and 1.2 cm in height and freeze-dried. The freeze-dried hydrogel samples were soaked in 100 mL 0.05 M phosphate buffer solutions (PBS) of different pH for 48 h. The samples of swollen hydrogel were weighed after removal of surface water using filter paper. And the swelling behavior of gelatin/CNCs composite hydrogel as a function of pH and CNCs content was studied. In this research, each group of data were measured three times and averaged. Results were calculated according to the following equation:

$$\text{Equilibrium water contents} = \frac{W_s - W_d}{W_d} \quad (1)$$

where *W<sub>s</sub>* is the mass of the hydrogel in the swollen state, *W<sub>d</sub>* is the mass of the hydrogel in the dried state.

Zeta potential measurements were performed at 25 °C using a Zetasizer Nano-ZS (Malvern Instruments, Westborough, MA, UK) capable of electrophoresis measurements. Dried hydrogel samples were ground to a diameter of ~25 μm by a cryogenic ball mill (Retsch CryoMill, Germany) and dissolved in the solution with the pH of 3, 4, 5, 7, 8, 9, 10, 11. The pH of 3, 4, 5, 7, 8 were phosphate buffer (0.05 M) and the pH of 9, 10, 11 were adjusted by 0.05 mol L<sup>-1</sup> NaOH. The grinding jar of the Cryo-Mill was continually cooled with liquid nitrogen from the integrated cooling system before and during the grinding process. The measurements were taken three times for each sample and average values were reported.

### 2.9. Cytotoxicity assays

The Hela cells were used to evaluate the cytotoxicity of the prepared gelatin-based hydrogels according to Cui *et al.*<sup>24</sup> In brief, the freeze-dried hydrogel samples were ground into a fine powder and sterilized by UV light for 2 h. Then, 30 mg of the sterilized powders were suspended in 5 mL PBS (pH 7.4) buffer for 12 h. The HeLa cells were seeded into 96 well plates at a density of 8 × 10<sup>3</sup> cells per well. Then 20 μL leaching solutions were added respectively and cultured in DMEM supplemented with 10% fetal bovine serum (FBS) at 37 °C in a humidified incubator. The optical density (OD) value was obtained by monitoring the absorbance of the broth at 570 nm with a microplate reader (Spectra Max M5, Molecular Devices, USA) and the viability of the Hela cells were detected by MTT method at different incubation times (12 h, 24 h and 48 h). The cell viability was calculated by normalizing the OD of samples to that of the control without any addition.

Additionally, cells were stained with a solution of fluorescein diacetate (FDA, 20 μg mL<sup>-1</sup>). The samples were observed using a fluorescence microscope (Olympus U-RFL-T, Japan).

## 3. Results and discussion

### 3.1. Analysis of thermostability

The TG and DTG curves of gelatin-based hydrogels were shown in Fig. 2 and values for the onset temperatures were taken from Fig. 2 and shown in Table 1. All samples exhibited two major



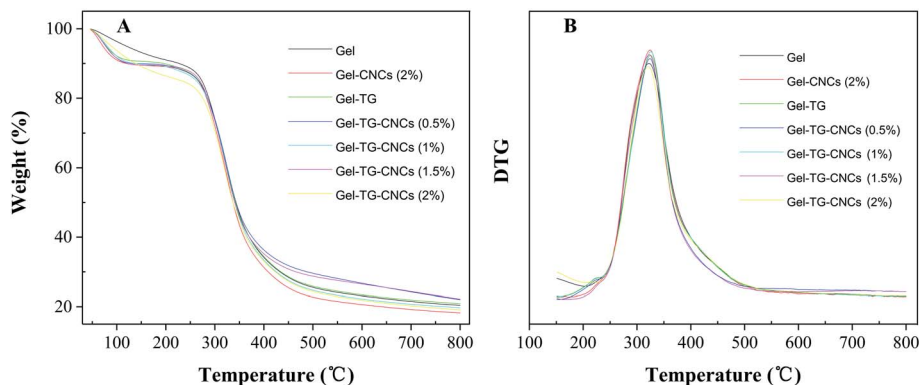


Fig. 2 TG (A) and DTG (B) thermograms of gelatin-based hydrogels with various amounts of CNCs content.

Table 1 The  $T_{\text{onset}}$  of gelatin-based hydrogels

Samples	$T_{\text{onset}}$ (°C)
Gel	206.3
Gel-CNCs (2%)	221.2
Gel-TG	230.3
Gel-TG-CNCs (0.5%)	231.6
Gel-TG-CNCs (1%)	232.5
Gel-TG-CNCs (1.5%)	233.9
Gel-TG-CNCs (2%)	235.2

mass loss stages in the temperature range of 45–800 °C. The first mass loss stage occurred approximately between 45 and 180 °C, which could be attributed to the loss of moisture (approximately 10%) in the freeze-dried hydrogels.<sup>25</sup> The onset decomposition temperature ( $T_{\text{onset}}$ ) of neat gelatin hydrogel (Gel) occurred at around 206 °C, which is association with the decomposition of collagen-like triple helix structure of gelatin.<sup>26</sup> It was observed that the onset temperature of the gelatin-based hydrogels increased with the increasing of CNCs content. Comparing with the pure gelatin hydrogel, the  $T_{\text{onset}}$  values of the Gel-CNCs (2%) and Gel-TG are up to 221.2 °C and 230.3 °C respectively. The results indicated that the addition of CNCs and mTG seemed to slightly increase the thermal stability of hydrogels. It could be related to the hydrogen bonding formation between CNCs and gelatin chains or the occurrence of crosslinking between gelatin chains.

### 3.2. XRD analysis

The crystal structure of CNCs, and the gelatin-based hydrogel samples characterized by XRD and are presented in Fig. 3. The X-ray diffractograms of CNCs show two typical characteristic diffraction peaks at  $2\theta = 18^\circ$  and  $22.5^\circ$ .<sup>27</sup> And the X-ray diffractograms of gelatin also show two typical characteristic diffraction peaks at  $2\theta = 8.5^\circ$  and  $20^\circ$ . According to Bigi's study, the peak at  $2\theta$  around  $8^\circ$  is related to the diameter of the triple helix and its intensity would be associated with the triple-helix content.<sup>28</sup> The broad peak at a  $2\theta$  value of approximately  $20^\circ$  corresponding to the amorphous nature of gelatin.<sup>29</sup> A

significant decrease in intensity of the peak at  $8.5^\circ$  of Gel-TG and Gel-TG-CNCs was depicted reflecting the decrease of the triple helix structure content. This result indicated that the covalent crosslinking between gelatin chains was performed by the addition of mTG, which decreased the crystalline intensity of gelatin. Similarly, the broad peak of at  $20^\circ$  of Gel-TG was also decreased. More broadly, with the addition of CNCs the peak at  $20^\circ$  almost disappeared (Gel-TG-CNCs). It was proved that the hydrogen bond between CNCs and gelatin chain have destroyed the close packing for the formation of regular crystallites, and this fact can improve the corresponding mechanical properties of the hydrogels.<sup>30</sup>

### 3.3. Analysis of rheological behavior

The storage modulus ( $G'$ ) which is an estimate of the strength of a material was obtained by oscillatory stress sweep method. As shown in Fig. 4A–C, the storage modulus of the gelatin-based hydrogels increased with the decreasing of temperature. Compared with the pure gelatin hydrogel, the storage modulus of those prepared by the addition of CNCs and/or mTG were

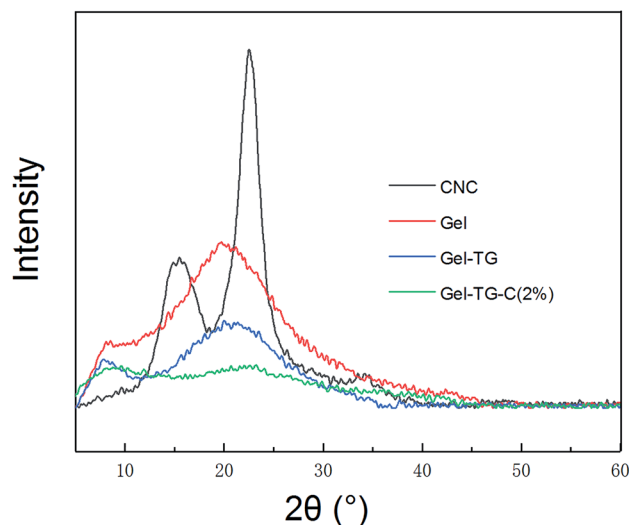


Fig. 3 XRD pattern of CNCs, gelatin, Gel-TG and Gel-TG-C (2%).





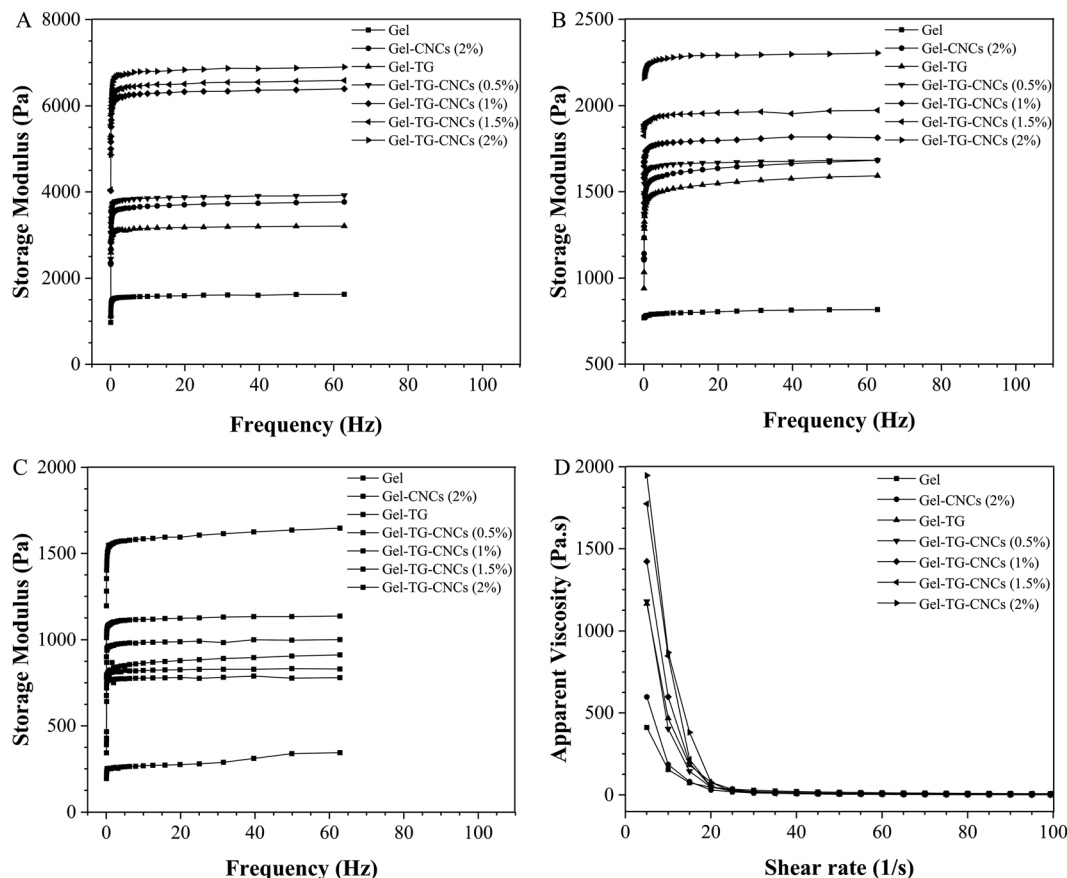


Fig. 4 The storage modulus of gelatin-based hydrogels at 5 °C (A), 15 °C (B) and 25 °C (C) during frequency sweep respectively, and apparent viscosity of gelatin-based hydrogels at 25 °C (D).

significantly increased. And for Gel-TG-CNCs, the storage modulus gradually increased with the increasing of CNCs content. As is known, mTG can catalyze the acyl transfer reaction to stimulate protein/peptide crosslinking and be widely used to improve the microstructural and rheological characteristics of gelatin-based hydrogels. Meanwhile, in these hydrogel samples, CNCs will serve as a nanofiller, have a certain specific surface area, quantum effect and surface effect, which caused the strength of the CNCs to blend with the softness of gelatin chains, thereby improving the mechanical strength of hydrogels.<sup>31</sup> Therefore, the storage modulus of Gel-TG-CNCs were higher than Gel-CNCs and Gel-TG, resulting from the dual reinforcing effect of CNCs and the covalent linkage catalyzed by mTG.

It can be seen from Fig. 4D, the viscosity of all hydrogels decreased rapidly with the increasing of shear rate, showing non-Newton behavior. Addition of CNCs into the polymer solution increased the apparent viscosity as is expected when solid particles are suspended in liquids. Microbial transglutaminase catalyzed the formation of cross-links between gelatin chains, producing higher molecular weights aggregation, thus resulting in increasing the initial apparent viscosity of Gel-TG. Obviously, Gel-TG show higher initial apparent viscosity value than Gel and Gel-CNCs (2%). This means that mTG

treatment seemed more efficiently increased the initial apparent viscosity than the addition of CNCs. It is notable that the initial apparent viscosity of the as-prepared Gel-TG-CNCs hydrogels strongly enhanced by the synergistic effect of mTG and CNCs. Moreover, for Gel-TG-CNCs hydrogels, with the increasing of CNCs content the shear thinning behavior became more obvious and the initial apparent viscosity increased. When the CNCs content increases from 0.5 to 2.0 wt%, the initial apparent viscosity is nearly fold. This may be due to CNCs benefited the forming of the network linked by some weak forces, such as hydrogen bonding.<sup>32</sup>

### 3.4. Gel breaking strength

Gel breaking strength is an important physical property of gelatin-base hydrogels in a wide range of applications, and depend heavily on the chemical structure of the hydrogels. The size of gelatin chains, triple helix content, degree of cross-linking and hydrogen bond between CNCs and gelatin play an important role in the gel strength.<sup>33</sup> The gel strength of gelatin-based hydrogels was shown in Fig. 5, CNCs and TG modified hydrogels showed higher gel strength than pure gelatin hydrogels. The gel strength of the Gel-CNCs (2%) was 3 times higher than that of pure gelatin hydrogels. This reinforced behavior can be ascribed to the uniformly dispensed CNCs particles in



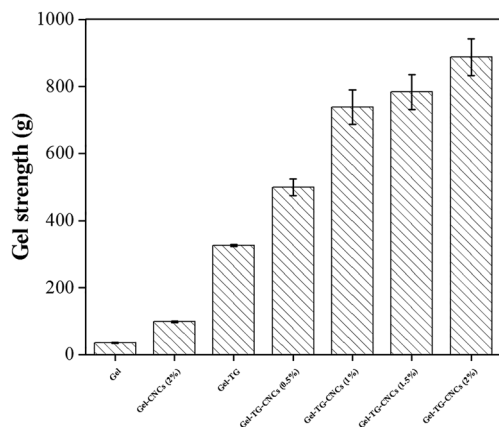


Fig. 5 The gel strength of gelatin-based hydrogels at 25 °C.

hydrogels, which can transfer the load from polymer chain to CNCs particles and avoid the growing of micro-cracks.<sup>34</sup> In addition, the improvement of the gel strength can also be attributed to the hydrogen bond between gelatin chain and CNCs particles, the same as other nanoparticles (CNTs) in gelatin hydrogels.<sup>35</sup> Moreover, the gel strength of Gel-TG was also significantly enhanced by forming the covalent cross-linking among gelatin chains. As expected, the simultaneous addition of CNCs and TG achieved a marked increasing in the gel strength compared with addition individual. It can be found

that the mechanical properties of Gel-TG-CNCs hydrogels depended not only on the reinforced behavior of CNCs particles, but also on CNCs/gelatin interactions and covalent cross-linking by mTG.

### 3.5. SEM

The morphology of the freeze-dried hydrogels was studied by SEM and the results were shown in Fig. 6. All hydrogels contained irregular porous structures with smooth pore walls. No CNCs can be clearly identified in the pore wall of the scaffold, which can be due to the good interfacial compatibility of the gelatin/CNCs composites. The pore dimension of Gel-TG was much smaller than that of pure gelatin hydrogels as seen from the images (Fig. 6a and b) at same magnification. This decrease in pore size was attributed to the crosslinking reaction among gelatin chains, which enhanced the interaction between the molecules, thereby making the internal structure of the hydrogel more compact. It is already reported that pore size of hydrogel decreases with degree of crosslinking.<sup>36</sup> After adding CNCs, the hydrogel samples have a more pronounced three-dimensional network structure (as shown in Fig. 6c–f), and this structure was probably associated with the supporting effect of CNCs on gelatin skeleton. Furthermore, the Gel-TG-CNCs show much bigger pore dimension than Gel-TG (all images at same magnification), and the pore dimension exhibited an increasing trend with increasing of CNCs content.

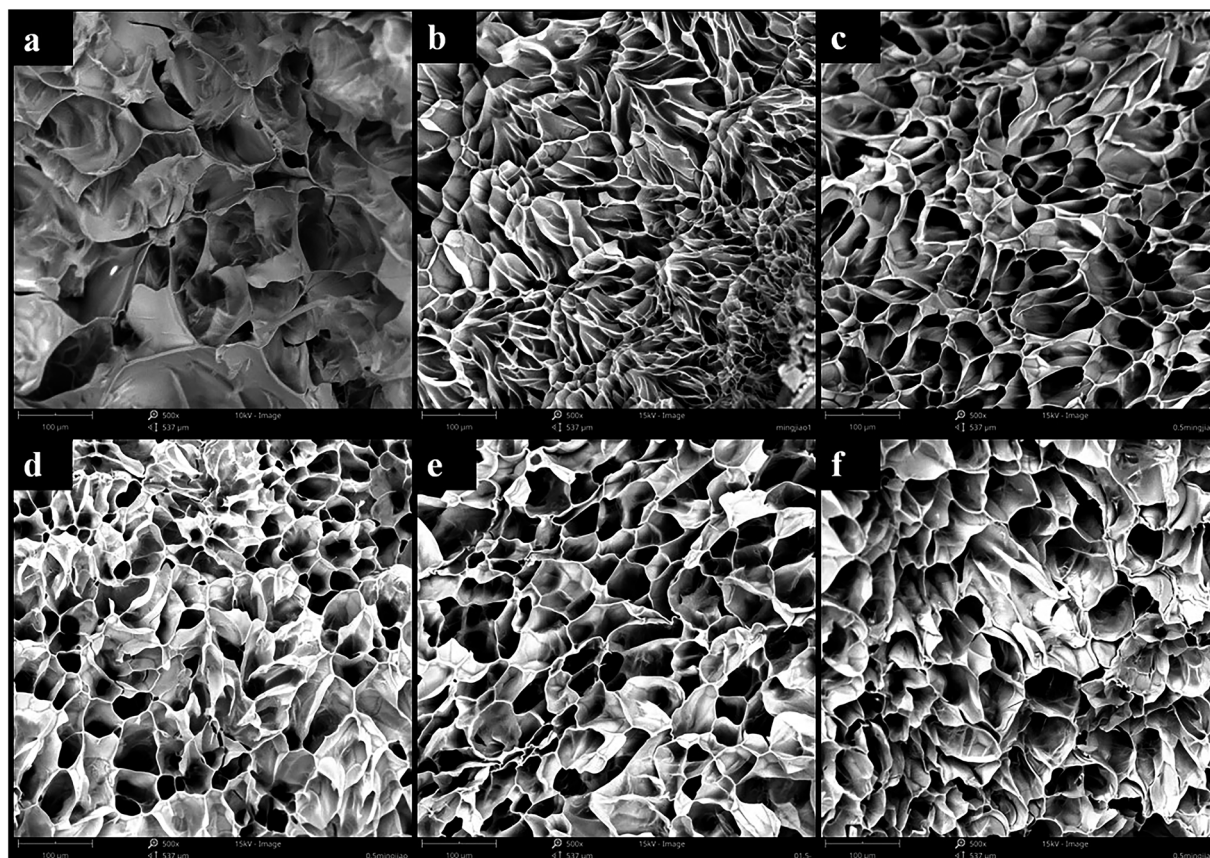


Fig. 6 SEM images of the (a) Gel, (b) Gel-TG, (c) Gel-TG-C (0.5%), (d) Gel-TG-C (1%), (e) Gel-TG-C (1.5%), (f) Gel-TG-C (2%).

For one thing, this trend occurred because the decreased degree of crosslinking due to the interference of CNCs particles. For another thing, incorporation of CNCs was expected to increase the rigidity of the hydrogel network, which decreases the shrinkage of the pore structures during freeze-drying process. Our result was approximately similar to that of Jiang *et al.*<sup>37</sup> and Xu *et al.*<sup>38</sup>

### 3.6. Swelling behavior

Swelling tests were performed to investigate the effect of pH on the swelling properties of the gelatin-based hydrogels. The equilibrium water contents of a variety of Gel-TG-CNCs are presented in Fig. 7A. The addition of CNCs seems to have little effect on the swelling behavior for the range of CNCs contents studied in this research. Furthermore, it is obvious that the equilibrium water contents of the hydrogel samples depend strongly on the pH values. All the hydrogel samples show the lowest swelling ratio at pH 7, which is nearby the isoelectric point of the Gel-TG-CNCs samples (Fig. 7B). Gelatin is amphoteric, it has both positive and negative charges on the molecule due to the presence of carboxylic and amino groups. The isoelectric point depends on the proportion of acidic and alkaline side chains of the amino acids on gelatin chain. As shown in Fig. 7B, the isoelectric point of type A gelatin is observed at pH 9.5, while the isoelectric point of Gel-TG-CNCs shift toward about 6.5. This can be explained by the decrease in the number of amino groups because of the crosslinking reaction catalyzed by mTG. At the isoelectric point, the electrical attraction between these opposite charges on gelatin chain will lead to network collapse, which result in the minimum swelling ratio.<sup>39</sup> When the pH of the swelling medium deviates from the isoelectric point, gelatin chains behave as polycations or polyanions, respectively. Then their swelling capacity increased. In addition, hydrogels under positive charge condition (below pI) have a higher equilibrium water contents than those that are negatively charged (above pI). Similar observations were reported by Ooi *et al.*<sup>39</sup> and Boral *et al.*<sup>40</sup>

### 3.7. Cytotoxicity

Cytotoxicity is one of the most important properties for biomaterials. The MTT test was chosen to evaluate the indirect

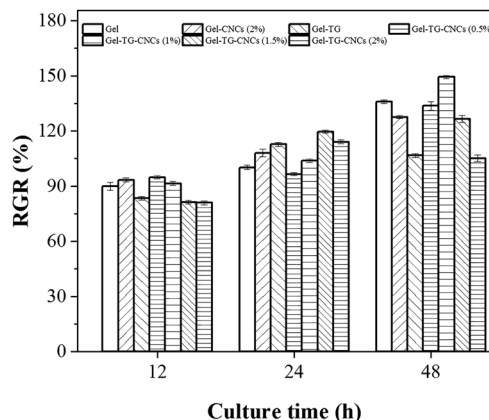


Fig. 8 Relative growth rate (RGR) of HeLa cells cultured in the leaching solution of gelatin-based hydrogels.

cytotoxicity of the hydrogels prepared in this study. As shown in Fig. 8, the MTT results of all hydrogels at different culture time (12 h, 24 h and 48 h) were resumed. Cell viability of all the hydrogels were higher than 80%, indicating their good cytocompatibility. Comparable cell viability values were reported by Yin *et al.*<sup>41</sup> and Asadi *et al.*<sup>42</sup> who use cellulose nanoparticles and gelatin to synthesis bio-hydrogel. The excellent cytocompatibility of the hydrogels was ascribed to the biocompatibility of the gelatin and CNCs, as well as the enzymatic approach of the hydrogels. Most importantly, the relative growth rate (RGR) of HeLa cells increased gradually over time and all samples were basically the same (Fig. 8), indicating that the cells proliferated well in the hydrogels. There are two possibilities to be suggested as the cause of the proliferation: (a) the gelatin skeleton can provide adhesion sites for cells, and the interaction between cells and gelatin chain further facilitated the proliferation,<sup>43</sup> or (b) the beneficial effect of collagen peptides in extraction solution which can promote cell growth and enhance cell proliferation.

As seen from Fig. 9, a large number of living cells were present and evenly distributed after 24 h of cell proliferation. The cells adhered well and proliferated on the culture plate without detectable changes in behavior. From Fig. 9a and b, we can clearly see that the appearance of cells maintained the

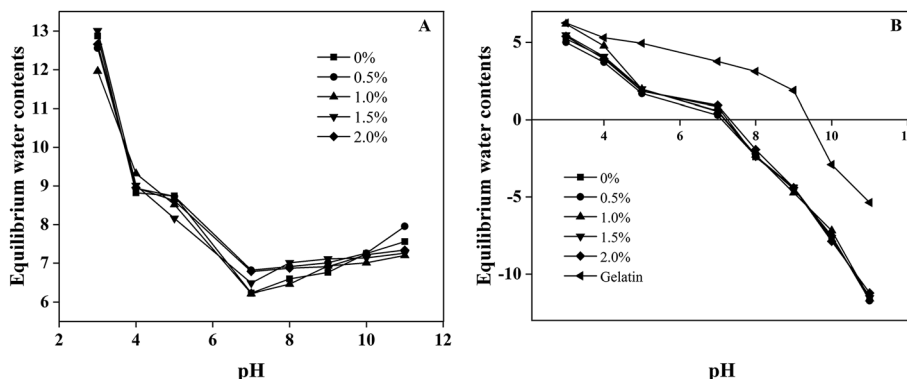


Fig. 7 (A) Swelling behavior of gelatin-based hydrogels at different pH. (B) The pI value of Gel-TG-C and gelatin.





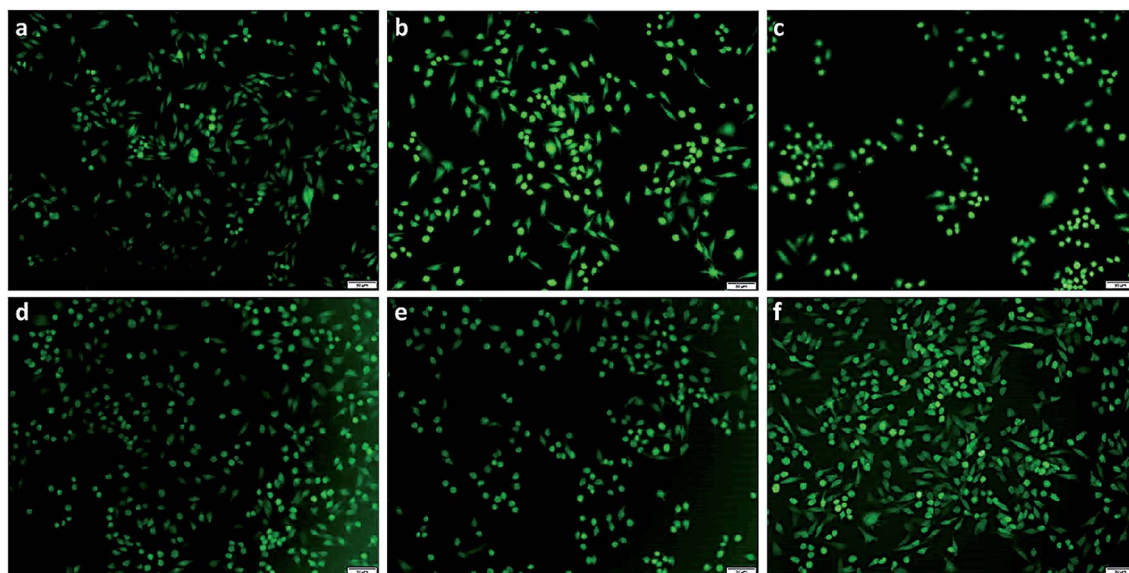


Fig. 9 The observation of HeLa cells by FDA staining after culturing for 24 hours. (a) Gel, (b) Gel-TG, (c) Gel-TG-CNCs (0.5%), (d) Gel-TG-CNCs (1%), (e) Gel-TG-CNCs (1.5%), (f) Gel-TG-CNCs (2%).

spindle morphology. And the number of living cells did not obviously decrease by the addition of CNCs content from 0.5 to 2.0 wt% (Fig. 9c–f), showing that the addition of mTG and CNCs did not induce detectable cytotoxicity. These pictures are consistent with the MTT results of cell viability (seen in Fig. 8). The above-mentioned results fully illustrated that these prepared gelatin-based hydrogels have good biocompatibility and low cytotoxicity.

## 4. Conclusion

In this study, a series of gelatin-based hydrogels were obtained by mTG cross-linking method and introducing CNCs as the strengthening agent. The physicochemical, mechanical, swelling, and cytocompatibility behaviors were investigated. It was founded that Gel-TG-CNCs exhibit higher storage modulus and breaking strength, and increasing CNCs concentrations led to better mechanical strength, which proved the dual reinforcing effect of CNCs and mTG. Most importantly, the results of MTT test demonstrated that the enzymatic cross-linking reaction and the introduction of CNCs had little toxicity to the cells. In conclusion, the enzymatically crosslinked gelatin/CNCs hydrogels are anticipated to have potential in the biomedical field such as drug delivery, wound repair and tissue engineering scaffolds.

## Conflicts of interest

There are no conflicts to declare.

## Acknowledgements

This work was financially supported by Shandong Provincial Key Research & Development Project (No. 2018GGX108006).

## References

- 1 H. Liu, C. Wang, C. Li, Y. Qin, Z. Wang, F. Yang, Z. Li and J. Wang, A functional chitosan-based hydrogel as a wound dressing and drug delivery system in the treatment of wound healing, *RSC Adv.*, 2018, **8**, 7533–7549.
- 2 A. D. Zhang, Y. Liu, D. Qin, M. J. Sun, T. Wang and X. G. Chen, Research status of self-healing hydrogel for wound management: a review, *Int. J. Biol. Macromol.*, 2020, **164**, 2108–2123.
- 3 D. Zhao, Q. Tang, Q. Zhou and K. Peng, A photo-degradable injectable self-healing hydrogel based on star poly(ethylene glycol)-*b*-polypeptide as a potential pharmaceuticals delivery carrier, *Soft Matter*, 2018, **14**, 7420–7428.
- 4 M. Zagórska-Dziok and M. Sobczak, Hydrogel-Based Active Substance Release Systems for Cosmetology and Dermatology Application: A Review, *Pharmaceutics*, 2020, **12**, 396.
- 5 A. Jayakumar, V. K. Jose and J. M. Lee, Hydrogels for Medical and Environmental Applications, *Small Methods*, 2020, **4**, 3.
- 6 F. Yin, L. Lin and S. Zhan, Preparation and properties of cellulose nanocrystals, gelatin, hyaluronic acid composite hydrogel as wound dressing, *J. Biomater. Sci., Polym. Ed.*, 2018, **30**, 190–201.
- 7 J. Jose, S. Sultan, N. Kalarikkal, S. Thomas and A. P. Mathew, Fabrication and functionalization of 3D-printed soft and hard scaffolds with growth factors for enhanced bioactivity, *RSC Adv.*, 2020, **10**, 37928–37937.
- 8 L. Deng, Y. Li, F. Feng and H. Zhang, Study on wettability, mechanical property and biocompatibility of electrospun gelatin/zein nanofibers cross-linked by glucose, *Food Hydrocolloids*, 2018, **87**, 1–10.
- 9 S. R. Radhika Rajasree, M. Gobalakrishnan, L. Aranganathan and M. G. Karthih, Fabrication and characterization of chitosan based collagen/gelatin composite scaffolds from





- big eye snapper *Priacanthus hamrur* skin for antimicrobial and anti oxidant applications, *Mater. Sci. Eng., R*, 2020, **107**, 110270–110271.
- 10 Z. Huang, Y. Z. Zhang, S. Ramakrishna and C. T. Lim, Electrospinning and mechanical characterization of gelatin nanofibers, *Polymer*, 2004, **45**, 5361–5368.
  - 11 R. Ardhani, I. D. Ana and Y. Tabata, Gelatin hydrogel membrane containing carbonate hydroxyapatite for nerve regeneration scaffold, *J. Biomed. Mater. Res., Part A*, 2020, **108**, 2491–2503.
  - 12 E. Matthew, G. R. A. Andres and N. C. Marin, Chemical and Enzymatic Protein Cross-Linking To Improve Flocculant Properties, *ACS Sustainable Chem. Eng.*, 2018, **6**, 12946–12952.
  - 13 X. Guo, Q. Zhou, P. Wang, Y. Yu and Q. Wang, Enzymatic crosslinking of silk sericin through combined use of TGase and the custom peptide, *J. Text. Inst.*, 2019, **111**, 84–92.
  - 14 T. Kashiwagi, K. I. Yokoyama, K. Ishikawa, K. Ono, D. Ejima, H. Matsui and E. I. Suzuki, Crystal Structure of Microbial Transglutaminase from *Streptovorticillium mobaraense*, *J. Biol. Chem.*, 2002, **277**, 44252–44260.
  - 15 Q. Liu, F. Qi, Q. Wang, H. Ding, K. Chu, Y. Liu and C. Li, The influence of particles size and its distribution on the degree of stress concentration in particulate reinforced metal matrix composites, *Mater. Sci. Eng., A*, 2018, **731**, 351–359.
  - 16 A. F. Loureno, J. A. Gamelas, P. Sarmiento and P. J. T. Ferreira, Enzymatic nanocellulose in papermaking – the key role as filler flocculant and strengthening agent, *Carbohydr. Polym.*, 2019, **224**, 115200.
  - 17 A. A. Adewunmi, S. Ismail and A. S. Sultan, Carbon Nanotubes (CNTs) Nanocomposite Hydrogels Developed for Various Applications: A Critical Review, *J. Inorg. Organomet. Polym.*, 2016, **26**, 717–737.
  - 18 Z. Zhang, Y. Liu, X. Chen and Z. Shao, Multi-responsive polyethylene–polyamine/gelatin hydrogel induced by non-covalent interactions, *RSC Adv.*, 2016, **6**, 48661–48665.
  - 19 Y. Piao and B. Chen, One-pot synthesis and characterization of reduced graphene oxide–gelatin nanocomposite hydrogels, *RSC Adv.*, 2016, **6**, 6171–6181.
  - 20 D. Varade and K. Haraguchi, Nanocomposite hydrogel as a template for synthesis of mono and bimetallic nanoparticles, *EXPRESS Polym. Lett.*, 2018, **12**, 996–1004.
  - 21 H. Wang, J. Li, X. Yu, G. Yan and L. Lin, Cellulose nanocrystalline hydrogel based on a choline chloride deep eutectic solvent as wearable strain sensor for human motion, *Carbohydr. Polym.*, 2021, **255**, 117443.
  - 22 R. Dash, M. Foston and A. J. Ragauskas, Improving the mechanical and thermal properties of gelatin hydrogels cross-linked by cellulose nanowhiskers, *Carbohydr. Polym.*, 2013, **91**, 638–645.
  - 23 K. J. De France, T. Hoare and E. D. Cranston, A Review of Hydrogels and Aerogels Containing Nanocellulose, *Chem. Mater.*, 2017, **29**, 4609–4631.
  - 24 X. Cui, J. L. Lee and W. N. Chen, Eco-friendly and biodegradable cellulose hydrogels produced from low cost okara: towards non-toxic flexible electronics, *Sci. Rep.*, 2019, **9**, 18166.
  - 25 Y. Zhao, Z. Li, W. Yang, C. Xue, Y. Wang, J. Dong and Y. Xue, Modification of Gelatine with *Galla chinensis* Extract, a Natural Crosslinker, *Int. J. Food Prop.*, 2016, **19**, 731–744.
  - 26 W. Ma, C. H. Tang, S. W. Yin, X. Q. Yang, Q. Wang, F. Liu and Z. H. Wei, Characterization of gelatin-based edible films incorporated with olive oil, *Food Res. Int.*, 2012, **49**, 572–579.
  - 27 Q. Xu, Y. Ji, Q. Sun, Y. Fu, Y. Xu and L. Jin, Fabrication of Cellulose Nanocrystal/Chitosan Hydrogel for Controlled Drug Release, *Nanomaterials*, 2019, **9**, 253.
  - 28 A. Bigi, S. Panzavolta and K. Rubini, Relationship between triple-helix content and mechanical properties of gelatin films, *Biomaterials*, 2004, **25**, 5675–5680.
  - 29 F. Liu, H. Majeed, J. Antoniou, Y. Li, Y. Ma, W. Yokoyama, J. G. Ma and F. Zhong, Tailoring physical properties of transglutaminase-modified gelatin films by varying drying temperature, *Food Hydrocolloids*, 2016, **58**, 20–28.
  - 30 H. Khanjanzadeh, R. Behrooz, N. Bahramifar, W. Gindl-Altmutter and T. Griesser, Surface chemical functionalization of cellulose nanocrystals by 3-aminopropyltriethoxysilane, *Int. J. Biol. Macromol.*, 2018, **106**, 1288–1296.
  - 31 W. Wang, X. Zhang, A. Teng and A. Liu, Mechanical reinforcement of gelatin hydrogel with nanofiber cellulose as a function of percolation concentration, *Int. J. Biol. Macromol.*, 2017, **103**, 226–233.
  - 32 M. Lotti, Ø. Gregersen, S. Moe and M. Lenes, Rheological Studies of Microfibrillar Cellulose Water Dispersions, *J. Polym. Environ.*, 2011, **19**, 137–145.
  - 33 S. Sinthusamran, S. Benjakul and H. Kishimura, Characteristics and gel properties of gelatin from skin of seabass (*Lates calcarifer*) as influenced by extraction conditions, *Food Chem.*, 2014, **152**, 276–284.
  - 34 M. K. Shin, G. M. Spinks, S. R. Shin, S. I. Kim and S. J. Kim, Nanocomposite Hydrogel with High Toughness for Bioactuators, *Adv. Mater.*, 2010, **21**, 1712–1715.
  - 35 S. R. Shin, H. Bae and J. M. Cha, Carbon Nanotube Reinforced Hybrid Microgels as Scaffold Materials for Cell Encapsulation, *ACS Nano*, 2012, **6**, 362–372.
  - 36 B. E. Mirzaei, S. A. A. Ramazani, M. Shafiee and M. Danaei, Studies on Glutaraldehyde Crosslinked Chitosan Hydrogel Properties for Drug Delivery Systems, *Int. J. Polym. Mater.*, 2013, **62**, 605–611.
  - 37 Y. Jiang, J. Zhou, H. Shi, G. Zhao, Q. Zhang, C. Feng and X. Xu, Preparation of cellulose nanocrystal/oxidized dextran/gelatin (CNC/OD/GEL) hydrogels and fabrication of a CNC/OD/GEL scaffold by 3D printing, *J. Mater. Sci.*, 2020, **55**, 2618–2635.
  - 38 Y. Zhu, F. Xu, Q. Liu, M. Chen, X. Liu, Y. Wang, Y. Sun and L. Zhang, Nanomaterials and plants: positive effects, toxicity and the remediation of metal and metalloid pollution in soil, *Sci. Total Environ.*, 2019, **662**, 414–421.
  - 39 S. Yin, O. Ishak, A. Mohd, C. Iqbal and M. Amin, Cellulose nanocrystals extracted from rice husks as a reinforcing material in gelatin hydrogels for use in controlled drug delivery systems, *Ind. Crops Prod.*, 2016, **93**, 227–234.
  - 40 S. Boral, A. N. Gupta and H. B. Bohidar, Swelling and deswelling kinetics of gelatin hydrogels in ethanol–water



- marginal solvent – ScienceDirect, *Int. J. Biol. Macromol.*, 2006, **39**, 240–249.
- 41 F. Yin, L. Lin and S. Zhan, Fabrication and In Vitro Evaluation of Nanocomposite Hydrogel Scaffolds Based on Gelatin/PCL-PEG-PCL for Cartilage Tissue Engineering, *J. Biomater. Sci., Polym. Ed.*, 2018, **30**, 190–201.
- 42 N. Asadi, E. Alizadeh, A. Rahmani Del Bakhshayesh, E. Mostafavi, A. Akbarzadeh and S. Davaran, Fabrication and In Vitro Evaluation of Nanocomposite Hydrogel Scaffolds Based on Gelatin/PCL-PEG-PCL for Cartilage Tissue Engineering, *ACS Omega*, 2019, **4**, 449–457.
- 43 T. Distler, K. McDonald, S. Heid, E. Karakaya and A. R. Boccaccini, Ionically and Enzymatically Dual Cross-Linked Oxidized Alginate Gelatin Hydrogels with Tunable Stiffness and Degradation Behavior for Tissue Engineering, *ACS Biomater. Sci. Eng.*, 2020, **6**, 3899–3914.

